Mechanical Response of Embryonic Stem Cells using Haptics-enabled Atomic Force Microscopy

Anand Pillarisetti[*], Carol Keefer[†], and Jaydev P. Desai[*]

[*]Robotics, Automation, Manipulation, and Sensing (RAMS) Laboratory
[†]Department of Animal and Avian Sciences
University of Maryland, College Park, USA

Abstract Mechanical manipulation and characterization of biological cells is currently one of the most exciting research areas in the field of medical robotics applied to cellular level interactions. While biologists are able to ascertain the change in cell status visually based on mRNA or proteins markers, it is often qualitative and difficult to quantitatively define the outcome of a cell progression during differentiation. Consequently, we propose to develop a haptics-enabled atomic force microscopy system to mechanically manipulate and characterize an individual cell. The haptic feedback interface proposed in this paper comprises of a PHANToM haptic feedback device combined with the atomic force microscope (AFM). The system has the capability of measuring forces in nN range and provides a haptic display of the cell indentation forces in real time. We conducted studies on mouse embryonic stem cells (mESC) and our experimental results indicate that the mechanical property of undifferentiated mESC differs from differenttiated mESC.

Introduction

Mechanical manipulation and characterization of biological cells is currently one of the promising research areas in the field of medical robotics applied to cellular level interactions. Several approaches are proposed in the literature to automate and improve the efficiency of cell manipulation systems. A detailed review on the existing techniques for cell manipulation is presented in [1]. One of the ways to improve the efficiency of biomanipulation tasks is the inclusion of force feedback [2, 3]. However, the experiments were performed on cells with dimensions in the range of 600 μm – 1 mm. On the other hand, in the field of cell biology most experiments involve cells with dimensions less than 100 μm. Mechanical characterization of cells can be used as a potential biological marker to detect its state [4]. For example, quantifying the mechanical behavior of stem cells may lead to effective regenerative therapies. Embryonic stem cells (ESC) have the unique capability to replace diseased or damaged tissue via cellular transplantation [5]; however, inducing targeted differentiation into specific tissue types in a controlled manner has proved to be problematic. Conventionally, biologists detect cell status visually based on mRNA or protein markers. These assays are often qualitative and do not quantitatively define the outcome of a cell progression during differentiation. Thus, we hypothesize that the mechanical property of undifferentiated mouse embryonic stem cells (mESC) differs from differentiated mESC in both live and fixed cells. To address this hypothesis, we have developed a haptics enabled atomic force microscope (AFM) system that can be used to manipulate cells and quantify their mechanical behavior. Robotics researchers have also proposed new human machine interfaces for nanomanipulation using AFM [6, 7]. However, the interfaces were not evaluated on biological systems. A nanomanipulation system consisting of an AFM and a haptic device has also been developed to provide force feedback from biological samples and carbon nanotubes [8]. In this set up the user does not feel the actual forces from the sample, but feels a surface representation that is simultaneously reconstructed during the AFM scan. In this paper, we present an AFM combined with haptic feedback to provide a means of mechanical phenotyping and monitoring live and fixed cells. The system has the capability to reflect cell indentation force in real-time to the user. Since, ESC have potential application in regenerative therapies, we chose to perform experiments on undifferentiated and differentiated mESC.

Materials and Methods

The haptic feedback interface consists of an Atomic Force Microscope (MFP-3D-BIO^{TM}, Asylum Research) and the PHANToM haptic feedback device (Sensable Technologies, Inc). The main part of AFM is the scan head which is integrated with a top view module and mounted on a active vibration isolation table manufactured by Herzan (see fig 1). The top view module enables viewing of cells and easy alignment of the laser beam on the AFM cantilever. XY stage (manual) allows the user to position the cell beneath the cantilever tip of AFM. The entire AFM set up is enclosed in a acoustic isolation chamber to prevent acoustic noise from interfering with the AFM measurements. The x and y-axes range of the scan head is 90 µm. The z-axis scan range is 40 µm. The AFM also has the capability to measure forces in the range of pN-nN. A v-shaped Pyrex Nitride cantilever (PNP-DB, NanoWorld AG) was used in our experiments. The spring constant of the cantilever was determined experimentally for each tip used in our studies using the IGOR software interface supplied by Asylum Research. The typical radius of curvature of the cantilever tip is below 10 nm.

The AFM system is used to obtain force and cell deformation data from biological samples. The cantilever is moved by the piezoelectric scanner in the z direction towards the cell. The deflection of the cantilever is detected by a photodiode when the tip comes in contact with the cell. When the tip of the cantilever is in contact with the cell, the initial cantilever deflection, d_0, and movement in z direction, z_0, are obtained (see fig 2). As the cantilever moves in the z direction and deforms the cell, the final cantilever deflection, d_1, and the movement, z_1, are obtained (see fig 2).

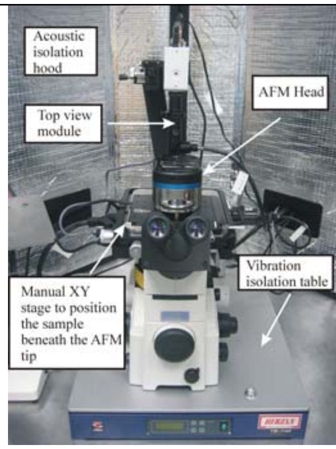

Fig 1. Experimental set for AFM imaging

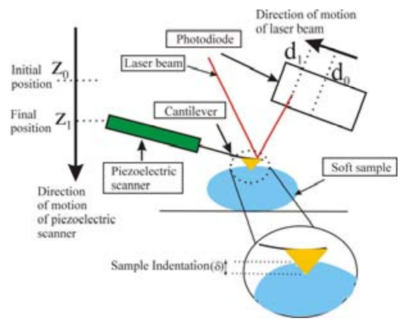

Fig 2. Schematic of AFM cantilever interacting with a cell. Point of contact: d_0 and z_0 represent the apparent cantilever deflection and movement respectively. The final cantilever deflection and movement are given by d_1 and z_1 respectively

The actual cantilever deflection, d, and the movement, z, are given by:

$$d = d_1 - d_0 \tag{1}$$

$$z = z_1 - z_0 \tag{2}$$

The difference between the actual cantilever movement, z, and actual cantilever deflection, d, represents the cell indentation, δ, and is given by (see fig 2):

$$\delta = z - d \tag{3}$$

Substituting (1) and (2) in (3) we get:

$$\delta = (z_1 - z_0) - (d_1 - d_0) \tag{4}$$

Thus the cell indentation, δ, can be used to compute the elastic modulus of the cell based on the Hertz contact model. The force exerted on a biological cell and the corresponding deformation predicts its mechanical behavior.

Cell Preparation

Mouse embryonic stem (ES) cells R1 (SCRC-1011, American Type Culture Collection [ATCC], Manassas, VA) were grown on 0.1% gelatin-coated plates in the absence of feeder cells. The ES medium consisted of 1000 U/ml leukemia inhibitory factor (LIF, ESGRO, Chemicon, Temecula, CA), 15% fetal bovine serum (FBS) (Invitrogen), and basic medium that included Knockout Dulbecco's modified Eagle's medium (Invitrogen), 2 mM L-glutamine, 1x non-essential amino acids, and 0.1 mM mercaptoethanol. Differentiation was induced by removal of LIF from the medium. Prior to experiments, cells were dispersed using trypsin to obtain single cells and were plated on 60 mm tissue culture petri dish. Fixed mouse ES cells were obtained by treating the live mouse ES cells with 4% formaldehyde for 10 minutes and were stored in phosphate buffered saline (PBS).

Mechanical characterization of a biological cell

The force exerted on a biological cell and the corresponding deformation predicts its mechanical behavior. Since the past decade, researchers have proposed different models to determine the mechanical properties of biological entities using AFM [9-11]. We are interested in quantifying the mechanical property of stem cells which would provide a better insight in developing an effective regenerative therapy. As an initial attempt towards this goal, we have used Hertz contact model to estimate the elastic modulus of undifferentiated and differentiated mESC in live as well as fixed states. The model assumes that: (a) the sample is elastic, isotropic, and homogenous, (b) the tip used for sample probing is infinitely stiff compared to the sample, and (c) no adhesion between the tip and the sample. For a conical tip indenting a sample, the relation between the indentation, δ, and the loading force (F) is given by [12]:

$$F = \frac{2E\tan(\alpha)}{\pi(1-\nu^2)}\delta^2 \tag{5}$$

where E and ν are the elastic modulus and Poisson’s ratio of the sample respectively. α is the opening angle of the conical tip and it was taken to be 35^o. The spring constant and the elastic modulus of the PNP- DB cantilever (NanoWorld AG) used in the indentation studies are 0.06 N/m and 222.22 Gpa respectively.

The Hertz contact theory models the tip as a cone. However, the actual geometry of the tip used in our studies is a pyramid. A contact model for a regular pyramid was developed by Bilodeau [13]. We used this model to compute the elastic modulus of mESC in interphase stage of the cell cycle process (please refer to Results section). The assumptions made in the Hertz theory are applicable in this analysis. For a tetrahedral pyramid, the force (F) versus indentation (δ) relationship is given by [13]:

$$F = \frac{8E\tan(\theta)}{9(1-\nu^2)}(\delta)^2 \tag{6}$$

The spring constant and the elastic modulus of AC240TS (Olympus, Inc) cantilever used to conduct studies on mESC in interphase stage are 2.00 N/m and 168.17 Gpa. The opening angle (α) of the tip is 35^0. Typically the elastic modulus of cells is in the range of kPa [14]. Hence the assumption (b) is valid in our analysis.

Haptic Interface

The force exerted on the cell and hence transmitted to the haptic feedback device is given by:

$$F = kd \tag{7}$$

where k is the spring constant of the cantilever obtained initially through the IGOR software after exciting the AFM scanning tip in various modes. Substituting (1) in (7), we get:

$$F = k(d_1 - d_0) \tag{8}$$

Thus, our haptics enabled AFM system obtains the relationship between the force exerted on the cell and the corresponding deformation. The force detected by the AFM during cell contact is acquired by a data acquisition board in real-time (model: dSPACE DS1103). The AFM is integrated with the PHANToM haptic feedback device and the interface allowed the user to feel the cell indentation force in real time. The force was amplified by a factor of 10^7 for the human operator to perceive the change in force during cell indentation by the AFM cantilever. Thus, haptics enabled AFM monitoring provides real time force information from an individual cell. This information can be used as a biological marker to detect the state of the cell.

Results

Our preliminary studies have involved indentation of live and fixed mESC. Through our preliminary studies, we have determined that undifferentiated (pluripotent) mESC has a more supple membrane. Fig 3(a) and (b) shows the force trigger curves for mESC where indentation force versus the cell indentation, δ, for differentiated and undifferentiated cells is shown for live and fixed mESC respectively. From the figure it is clear that undifferentiated mESC in each category is more elastic compared to differentiated mESC. These studies were done for a controlled 1μm deflection of the AFM tip during cell indentation. Through our haptic feedback interface described in the previous section, we are able to provide force feedback to the user in real-time and "feel" the change in the cell stiffness as the AFM tip indents on the cell surface.

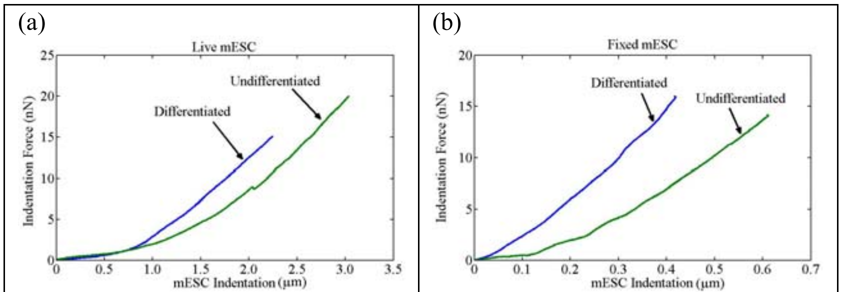

Fig 3. Force trigger curves for mESC where indentation force versus the cell indentation for differentiated and undifferentiated cells is shown for (a) live mESC and (b) fixed mESC

Single indentation studies on live and fixed cells

Using the peak trigger force for 1μm deflection of the AFM tip during cell indentation obtained from the previous study for live and fixed – differentiated and undifferentiated mESC cells, we performed several mESC indentation tasks using the peak trigger force as the trigger value in AFM studies.

Fixed Cells

Fig 4 and fig 5 shows the force versus cell indentation, δ, for fixed differentiated mESC and fixed undifferentiated mESC respectively. Based on the experimental data, we performed a least square fit on the dataset and the corresponding least square fit is shown in the figure. The R^2 value for fixed differentiated mESC was found to be 0.5816 and R^2 value for fixed undifferentiated mESC was found to be 0.6453. Fig 6 shows the average elastic modulus of the cell membrane for fixed differentiated (100.01 kPa) and undifferentiated (18.923 kPa) mESC. Equation (5) was used to compute the elastic modulus of the cell membrane for each mESC indentation task by assuming Poisson's ratio of 0.5.

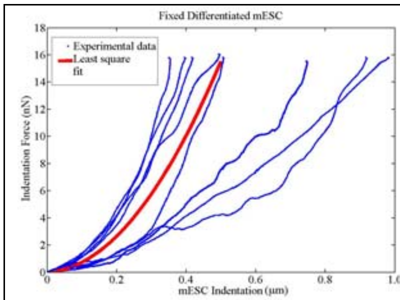

Fig 4. Force (F) versus cell indentation (δ) for fixed differentiated mESC. The R^2 value for the least square fit is 0.5816.

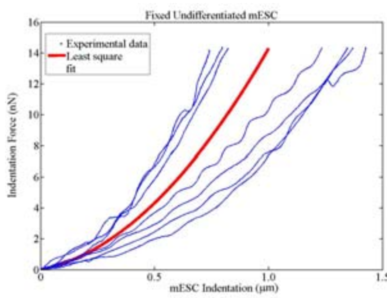

Fig 5. Force (F) versus cell indentation (δ) for fixed undifferentiated mESC. The R^2 value for the least square fit is 0.6453.

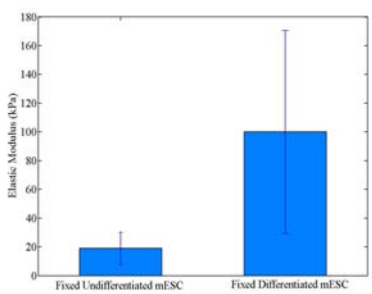

Fig 6. Elastic modulus of fixed mESC calculated from the Hertz contact model along with the error bar.

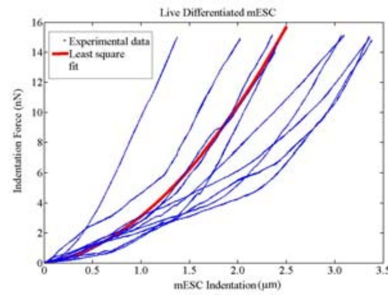

Fig 7. Force (F) versus cell indentation (δ) for live differentiated mESC. The R^2 value for the least square fit is 0.5059.

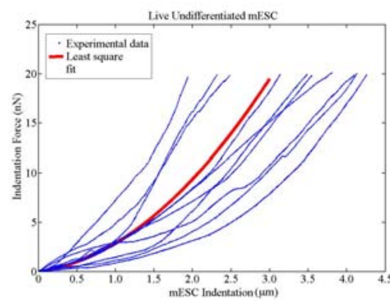

Fig 8. Force (F) versus cell indentation (δ) for live undifferentiated mESC. The R^2 value for the least square fit is 0.6102.

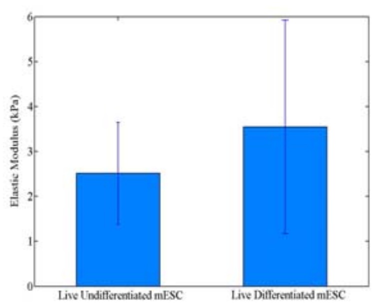

Fig 9. Elastic modulus of live mESC calculated from the Hertz contact model along with the error bar.

The standard deviation is 11.071 kPa and 70.581 kPa for fixed undifferentiated and differentiated mESC respectively. We also performed a 2-way ANOVA analysis on the elastic modulus values for differentiated and undifferentiated fixed mESC and the p-value obtained was 0.0334.

Live Cells

Fig 7 and fig 8 shows the force versus cell indentation, δ, for live differentiated mESC and live undifferentiated mESC respectively. Similar to the fixed cells analysis, we performed a least square fit on the dataset and the corresponding least square fit is shown in the figure. The R^2 value for live differentiated and undifferentiated mESC was found to be 0.5059 and 0.6102. Fig 9 shows the average elastic modulus of the cell membrane for live differentiated (3.546 kPa) and undifferentiated (2.516 kPa) mESC. Equation (5) was used to compute the elastic modulus of the cell membrane for each mESC indentation task by assuming Poisson's ratio of 0.5. The standard deviation was 1.1332 kPa and 2.3771 kPa for live undifferentiated and differentiated mESC respectively. We also performed a 2-way ANOVA analysis on the elastic modulus values for differentiated and undifferentiated live mESC and the p-value obtained was 0.0861.

The large standard deviation in elastic modulus for both live and fixed cells could be due to the variation in the stage of the cell cycle at the time of cell indentation. The cell cycle consists of four distinct phases: G1 phase, S phase, G2 phase, and M phase. G1, G2, and S phases are considered the interphase, while M phase comprises the process of mitosis and cytokinesis (cell division) which results in the formation of two daughter cells. During cell indentation studies, it is difficult to ascertain the stage of cell cycle. This could explain the large variation in the elastic modulus value for live and fixed cells. As a result we performed experiments on mESC in interphase stage of the cell cycle process

Live cells in interphase stage

Fig 10 and Fig 11 shows the force (F) versus cell indentation, δ, for live differentiated and live undifferentiated mESC in interphase stage respectively. We performed Bilodeau model fit on the data as shown in the figure. The R^2 value for live differentiated and undifferentiated mESC was found to be 0.85 and 0.90 respectively. Fig 12 shows the average elastic modulus of live differentiated (16.06 kPa) and undifferentiated (1.49 kPa) mESC. Equation (6) was used to compute the elastic modulus of the cell membrane for each mESC indentation task by assuming Poisson's ratio of 0.5. The standard deviation was 0.314 kPa and 4.705 kPa for live undifferentiated and differentiated mESC respectively. Thus we obtain a low deviation in modulus compared to the results shown in fig 6. We also performed Kruskal-Wallis statistical test on the elastic modulus values for differentiated and

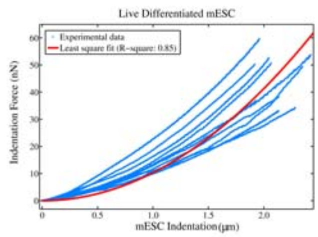

Fig 10. Force (F) versus cell indentation (δ) for live differentiated mESC (interphase stage)

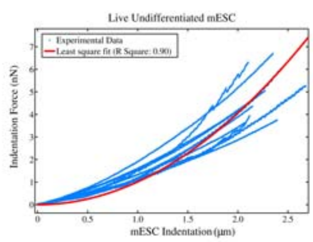

Fig 11. Force (F) versus cell indentation (δ) for live undifferentiated mESC (interphase stage)

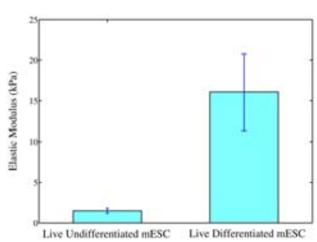

Fig 12. Elastic modulus of live mESC (interphase stage) calculated from the Bilodeau contact model along with error bar.

undifferentiated live mESC and the p-value obtained was 0.0002, leading to a probability of greater than 99.98% that there was a significant difference between the data sets.

Discussion

In this paper, we have presented our preliminary work towards the development of a haptics enabled atomic force microscopy system for mechanical phenotyping of live and fixed cells in differentiated and undifferentiated states. The haptic feedback obtained during cell indentation by the AFM tip was in real-time and the subject was able to feel the change in the stiffness during cell deformation. We did several trials on live as well as fixed cells for single indentation tasks and used the force curves obtained from each experiment to deduce the elastic modulus of the cell membrane using the Hertz contact model. However, a large deviation in elastic modulus was observed from the initial studies which could be due to the variation in the stage of the cell cycle (M-phase or interphase) at the time of cell indentation. As a result we performed experiments on mESC in interphase stage of the cell cycle process and obtained a lower deviation in elastic modulus (computed from Bilodeau model) as well as a significant statistical difference between undifferentiated and differentiated mESC in live cells (p-value= 0.0002 from Kruskal-Wallis test). We have also performed experiments on fixed cells in interphase stage and obtained promising results [15].

The approach presented in this paper could be used to develop improved methods of targeted cellular differentiation of human embryonic and/or adult stem cells for therapeutic purposes, for development of new diagnostic procedures, and to monitor cellular responses to environmental stimuli.

Acknowledgments: We acknowledge the support of National Science Foundation grant 0711038 for this work.

References

1] J. P. Desai, A. Pillarisetti, and A. D. Brooks, "Engineering Approaches to Biomanipulation," Annual Review of Biomedical Engineering35-53, 2007.
[2] Z. Lu, P. C. Y. Chen, J. Nam, R. Ge, and W. Lin, "A micromanipulation system with dynamic force-feedback for automatic batch microinjection," Journal of micromechanics and microengineering, vol. 17314-321, 2007.
[3] A. Pillarisetti, M. Pekarev, A. D. Brooks, and J. P. Desai, "Evaluating the Effect of Force Feedback in Cell Injection," IEEE Transactions on Automation Science and Engineering, vol. 4(3), pp. 322-331, 2007.
[4] G. Y. H. Lee and C. T. Lim, "Biomechanics approaches to studying human diseases.," Trends in Biotechnology vol. 25(3), pp. 111-118, 2006.
[5] A. G. Smith, "Embryo-derived stem cells: of mice and men," Annual review of cell and developmental biology, vol. 17435-462, 2001.
[6] M. Sitti and H. Hashimoto, "Tele-Nanorobotics Using Atomic Force Microscope," presented at International Conference on Inteligent Robots and Systems, Victoria, B.C.,Canada, 1739-1746, 1998.
[7] W. Vogl, M. Sitti, and M. F. Zah, "Nanomanipulation with 3D visual and force feedback using atomic force microscope," in 4th IEEE Conference on Nanotechnology, 2004, pp. 349-351.
[8] M. Guthold, M. R. Falvo, W. R. Matthews, S. Paulson, S. Washburn, D. A. Erie, S. R., F. P. Brooks, Jr., and R. I. Taylor, "Controlled Manipulation of Molecular samples with the nano-Manipulator," IEEE/ASME Transactions on Mechatronics, vol. 5(2), pp. 189-197, 2000.
[9] J. H. Hoh and C. Schoenenberger, "Surface morphology and mechanical properties of MDCK monolayers by atomic force microscopy," Journal of Cell Science, vol. 1071105-1114, 1994.
[10] Q. H. Qin and M. V. Swain, "A micro-mechanics model of dentrin mechanical properties " Biomaterials, vol. 255081-5090, 2004.
[11] W. Xu, P. J. Mulhern, B. L. Blackford, M. H. Jericho, and I. Templeton, "A new atomic force microscopy technique for the measurement of the elastic properties of biological materials," Scanning Microscopy, vol. 8499-506, 1994.
[12] A. C. Fischer-Cripps, Introduction to contact mechanics, Second ed. New York: Springer, 2007.
[13] G. G. Bilodeau, "Regular pyramid punch problem," Journal of applied mechanics, vol. 59519 - 523, 1992.
[14] J. L. Alonso and W. H. Goldmann, "Feeling the forces: atmoic force microscopy in cell biology," Life Sciences, vol. 722553 - 2560, 2003.
[15] A. Pillarisetti, C. Keefer, and J. P. Desai, "Mechanical Characterization of Fixed Undifferentiated and Differentaited mESC," in International Conference on Biomedical Robotics and Biomechatronics Scottsdale, Arizona, 2008 (accepted).